

# Vibrational Dephasing of Long- and Short-Lived Primary Donor Excited States in Mutant Reaction Centers of *Rhodobacter sphaeroides*<sup>†</sup>

Marten H. Vos,<sup>\*,‡</sup> Michael R. Jones,<sup>§</sup> Jacques Breton,<sup>||</sup> Jean-Christophe Lambry,<sup>‡</sup> and Jean-Louis Martin<sup>‡</sup>

Laboratoire d'Optique Appliquée, INSERM U451, CNRS URA 1406, Ecole Polytechnique-ENSTA, 91120 Palaiseau, France, Krebs Institute for Biomolecular Research and Robert Hill Institute for Photosynthesis, Department of Molecular Biology and Biotechnology, University of Sheffield, Western Bank, Sheffield, S10 2UH, United Kingdom, and SBE/DBCM, CEN de Saclay, 91191 Gif-sur-Yvette Cedex, France

Received September 12, 1995; Revised Manuscript Received December 7, 1995<sup>⊗</sup>

**ABSTRACT:** Femtosecond spectroscopy was used to study vibrational dynamics in the first singlet excited state (P\*) of the primary donor of bacterial reaction centers (RC) in which primary electron transfer dynamics have been altered by single amino acid modifications. We studied intracytoplasmic RC-only membranes containing *Rhodobacter sphaeroides* wild-type RCs and RCs bearing mutations in the vicinity of P, where Tyr M210 was modified to His, Leu, and Trp and where Phe L181 was modified to Tyr. These mutations do not change the frequencies of the main low-frequency activated modes, which is consistent with a description in which these modes involve extended regions of the protein. Electron transfer in FL181Y, YM210H, and wild-type RCs at 10 K occurs in ~1 ps or less, and the damping of the coherences occurs simultaneously with the decay of the P\* excited state. These results, and a comparison with YM210L RCs, show that in wild-type RCs the damping is primarily determined by the depletion of P\* and not by vibrational dephasing induced by interactions with the bath or nonharmonic coupling. In the YM210L and W mutants, electron transfer occurs on a time scale of hundreds of picoseconds at 10 K. Analysis of the longer-lasting vibrational dynamics in these mutants sets a new *lower limit* for the intrinsic vibrational dephasing time of 1.2 ps for some modes, but of ~2 ps for most activated modes.

Localized external perturbations in proteins, such as ligand binding to a specific site or capture of a photon by pigment cofactors, may induce delocalized conformational changes of functional importance. These changes are brought about by the activation of low-frequency vibrational modes. Light-activated proteins are particularly suitable to study such motions in real-time using ultrafast spectroscopic techniques. Stimulated emission studies (Vos et al., 1991, 1993, 1994a,b) and very recently also spontaneous emission studies (Stanley & Boxer, 1995) have shown that photon capture by the bacterial reaction center (RC) activates low-frequency vibrational motions of specific frequencies in the excited state (P\*) of the primary electron donor that maintain phase relationships on the time scale of the primary electron transfer (ET) process, at low temperature as well as at room temperature. This constitutes an example of a regime of vibrational coherence during a biological reaction. Vibrational coherence has now also been observed in other light-sensitive proteins: in photosynthetic antenna proteins under conditions where their origin could not be unambiguously assessed (Chachisvilis et al., 1994; Savikhin et al., 1994) and in the photoisomerized bathorhodopsin state of rhodopsin (Wang et al., 1994).

For wild-type (WT) RCs at low temperature, the Fourier transform (FT) spectrum of the induced vibrational motions displays a series of low-frequency bands, and the oscillations can be observed up to ~2 ps; i.e., they damp concomitantly

with the depletion of P\* by ET, which is also nearly completed in 2 ps. The vibrational motions are monitored by means of oscillations of the shape of the stimulated emission band. In principle, damping of the observed oscillations may have two origins: depletion of the P\* state via ET or vibrational dephasing arising from coupling to the bath. A way to estimate the intrinsic dephasing time is to study mutant RCs in which the speed of ET is affected but where there is negligible modification of the vibrational pattern. The P\* state is long-lived in the previously studied D<sub>LL</sub> mutant of *Rhodobacter capsulatus* (Breton et al., 1990), where the symmetrization of an entire  $\alpha$ -helix resulted in the loss of the acceptor bacteriopheophytin molecule H<sub>L</sub>. However, a detailed comparison between WT RCs and RCs from this mutant is complicated by the strongly perturbed electronic and vibrational spectra observed in the latter (Vos et al., 1993).

In this paper, we address the question of the relation between ET and observed dephasing by studying a series of mutants with altered ET characteristics but which exhibit minimal structural perturbations. The mutants studied, from *Rhodobacter sphaeroides*, contain single-site alterations of the tyrosine at position M210, located in the vicinity of P (the bacteriochlorophyll dimer donor), H<sub>L</sub> (the bacteriopheophytin acceptor), and B<sub>L</sub> (the intermediately located bacteriochlorophyll monomer), and the symmetry-related phenylalanine at position L181. Such mutations alter the P<sup>+</sup>/P redox potential and the rate of primary ET (Jia et al., 1993; Nagarajan et al., 1993). They may also alter the redox properties of the other chromophores and their electronic

<sup>†</sup> M.R.J. is a BBSRC Senior Research Fellow.

<sup>‡</sup> Ecole Polytechnique-ENSTA.

<sup>§</sup> University of Sheffield.

<sup>||</sup> SBE/DBCM, CEN de Saclay.

<sup>⊗</sup> Abstract published in *Advance ACS Abstracts*, February 1, 1996.

couplings. However, the changes in the ground state electronic spectra (Gray et al., 1990; Jones et al., 1994) and the intradimer charge distribution in P<sup>+</sup> (Jones et al., 1994) are minor, and these residues are probably not involved in hydrogen bonding with the chromophores. For isolated RCs of one such mutant, YM210F, the vibrational spectrum of activated modes monitored by spontaneous emission experiments was indeed observed to be similar to WT (Stanley & Boxer, 1995), which is consistent with a minimal structural perturbation.

Several femtosecond studies on detergent-isolated RCs from *R. sphaeroides* and *R. capsulatus* with mutations at the M210 (M208 for *R. capsulatus*) and L181 positions have been reported (Finkel et al., 1990; Nagarajan et al., 1990, 1993; Chan et al., 1991; Jia et al., 1993; Hamm et al., 1993; Shochat et al., 1994). In most cases, the primary ET reaction is slower than that observed in WT RCs, by as much as 2 orders of magnitude for the YM210W mutant at 80 K (Nagarajan et al., 1993). In contrast, in the FL181Y mutant of *R. capsulatus* and *R. sphaeroides*, ET is speeded up from ~3.5 ps in WT to ~2.1 ps, at room temperature (Jia et al., 1993; Hamm et al., 1993). The series of four mutants studied here contain RCs with both slower and faster ET than WT. It is shown that the damping of the oscillations reflecting coherent nuclear motions is limited by the ET time in the WT RC and those mutant RCs that exhibit a fast rate of ET. These results yield a new lower limit for the intrinsic vibrational dephasing time in RCs.

This work was performed on intracytoplasmic membranes from antenna-deficient "RC-only" bacterial strains. In membrane-bound WT RCs, the dephasing of the vibrational coherence features is slightly slower than in detergent-isolated RCs (Vos et al., 1994c). The experiments were carried out at 10 K, where the vibrational motions are most clearly resolved. A significant experimental improvement, essential for the careful screening of series of mutants, has been the implementation of a fast read-out CCD camera for signal detection, which allows for a much faster and more complete data collection than is possible when using single diodes.

## MATERIALS AND METHODS

The construction of the mutant reaction centers bearing changes at the M210 position to Leu and His has been described previously (Jones et al., 1994). The changes Tyr M210→Trp and Phe L181→Tyr were made in a similar manner, using in the case of the latter change a 0.85 kb *Xba*I–*Sal*I restriction fragment encompassing the *puf*L gene as the template for mutagenesis. Codon changes were TTC→TAC (Phe L181→Tyr) and TAC→TTC (Tyr M210→Trp). The deletion and expression systems used to construct mutants with a reaction center-only phenotype are described in detail in Jones et al. (1992). The growth of mutant strains of *R. sphaeroides* and the preparation of intracytoplasmic membranes for spectroscopy were as described in Jones et al. (1994). It should be noted that this study was carried out on membrane-bound reaction center complexes. Recent experiments have shown that the membrane environment has a small influence on the characteristics of electron transfer (Vos et al., 1994c; Beekman et al., 1995).

The membranes were suspended in 20 mM Tris buffer, pH. 8.0, and were mixed with 50% glycerol (v/v). The

Table 1: Characteristics of P Absorption and P\* Decay at 10 K

	$\lambda_{\max}(\text{P})$ (nm)	$\lambda_{\max}(\text{SE})$ (nm) <sup>a</sup>	$\tau_1$ (ps) <sup>b</sup>	$\tau_2$ (ps)	$A_1$ (%) <sup>c</sup>	QY(P <sup>+</sup> ) <sup>d</sup>
WT	892	923	1.1	7	90	1.0
YM210L	895	924	190		100	0.7
YM210W	890	922	320		100	0.5
YM210H	895	924	1.2	20	75	1.0
FL181Y	893	924	0.7	2.0	90	1.0

<sup>a</sup> Estimated from the disappearance of fundamental frequency oscillatory features. <sup>b</sup> Best fits from the kinetics of P\* decay at the emission maximum. Kinetic traces of 300 ps full scale (YM210L and YM210W) and both 4 and 50 ps full scale (others) were used. <sup>c</sup> Percentage of the fast component ( $\tau_1$ ). <sup>d</sup> Quantum yield for P<sup>+</sup> formation estimated from the decay kinetics at 870 nm (P bleaching) during charge separation. This value should be considered as only a rough estimate ( $\pm 0.1$ ) in view of the limited kinetic window (300 ps) and the possibility of spectral evolution not related to population decay (Nagarajan et al., 1993; Peloquin et al., 1995).

concentration of the sample was adjusted to an optical density of ~0.4 at 880 nm (optical path length 1 mm); 50 mM dithiothreitol was added to prereduce the quinone electron acceptor Q<sub>A</sub>. The measurements were performed at 10 K in a convection cryostat.

The arrangement of the femtosecond spectrometer was as described previously (Vos et al., 1994a) with the following modifications. (1) The ~30 fs pump pulses were centered at 880 nm, by using the dye LDS 867 in mixtures of methanol, ethanol, and propylene carbonate as an amplification medium for the continuum. (2) The probe beam was compressed using a pair of F2 prisms, resulting in an essentially chirp-free (20 fs) continuum over the wavelength range 880–960 nm. The chirp was measured by monitoring the bleaching of the P-band of *Rhodospseudomonas viridis* RCs (Vos et al., 1994a) or the induced birefringence in CS<sub>2</sub> with identical results. (3) The transmission of the test and reference probe beams after passing the monochromator was monitored with an EG&G OMA4 CCD camera. The readout time of this camera is fast enough to allow shot-to-shot normalization at the repetition rate of our laser (30 Hz) of entire spectra with a resolution of ~1 nm. The data were analyzed by Fourier transformation with a resolution of 8 cm<sup>-1</sup> of the oscillatory parts as described (Vos et al., 1994a).

## RESULTS

The time evolution of the transient absorption spectra in the 850–1000 nm near-infrared region was monitored for WT RCs and the four mutant complexes on a 4 ps time scale to obtain the oscillatory features and either on a 50 ps or a 300 ps time scale to get a more complete picture of the overall decay of P\*. All of the mutant RCs displayed oscillatory features in the stimulated emission spectral region (observed as an apparent additional "bleaching" at the red side of the bleach of the ground state absorption band of P in these experiments), similar to those of WT RCs (Vos et al., 1994a). The low-temperature ground state absorption maxima of P and the stimulated emission maxima, estimated from the disappearance of the fundamental frequency features (Vos et al., 1993), were all very similar (Table 1), facilitating comparison between the mutants. The time scales of the decay of P\*-stimulated emission differ by 2–3 orders of magnitude among the mutants, in general agreement with previous measurements, mostly at higher temperatures, on isolated RCs of *R. sphaeroides* and *R. capsulatus* (Finkel

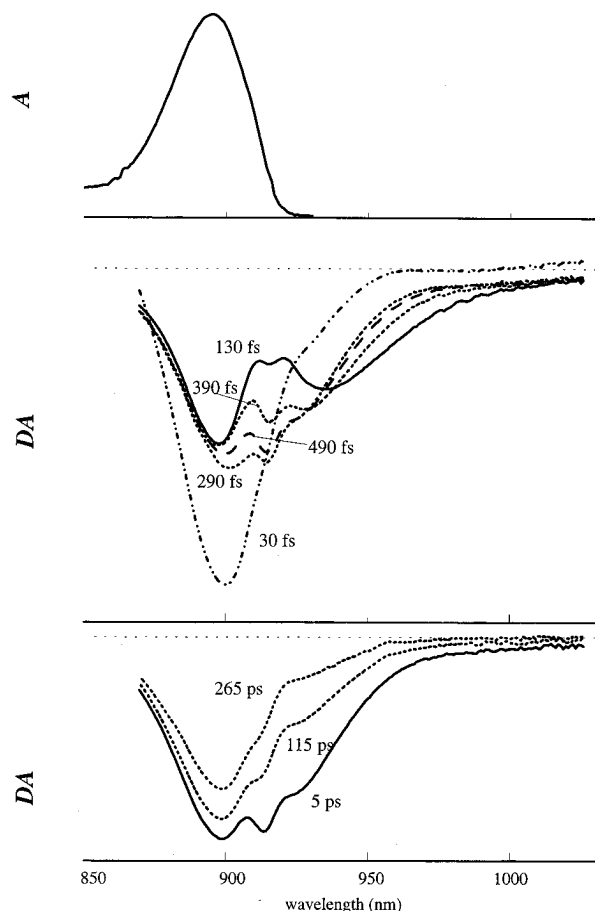


FIGURE 1: 10 K ground state absorption spectrum of RC-only membranes from the YM210L mutant obtained with the femto-second continuum in the absence of a pump pulse (upper panel) and transient absorption spectra at various delay times between pump and probe pulse (lower panels).

et al., 1990; Nagarajan et al., 1990, 1993; Chan et al., 1991; Jia et al., 1993; Hamm et al., 1993; Shochat et al., 1994). Table 1 gives fit parameters of the decay as measured at the center of the emission band. The fit parameters should be considered as approximate  $P^*$  decay times as, even at the center of the band, oscillatory components are superimposed on the decay (Vos et al., 1993, 1994a; Jean, 1994) and furthermore a time-dependent blue-shift of the emission band occurs in all of the mutants and in the WT [cf. Nagarajan et al. (1993) and Vos et al. (1994b)]. For the long-lived mutants (YM210L and YM210W), the decay at the extreme blue side of the ground state absorption band, where no stimulated emission is expected at longer times, indicates recovery of the ground state of P on the time scale of  $P^*$  decay. Thus, under these conditions, ET is so slow that its quantum yield substantially decreases.

Figure 1 shows the transient spectra at various delay times for the YM210L mutant. For this mutant, the decay of  $P^*$  at 10 K occurs on the time scale of hundreds of picoseconds (fitted decay time 190 ps at 924 nm, Table 1). The characteristic features of the early-time transient spectra (including three apparent minima at  $\sim 895$ , 910, and 925 nm) also decay on this time scale toward a transient spectrum dominated by the bleaching of the P ground state band at 895 nm. The extent of the spectral modulations varies somewhat between the five types of RCs studied.

For the YM210L (and also YM210W) mutant, no overall decay of the  $P^*$  state occurs on the time scale of a few

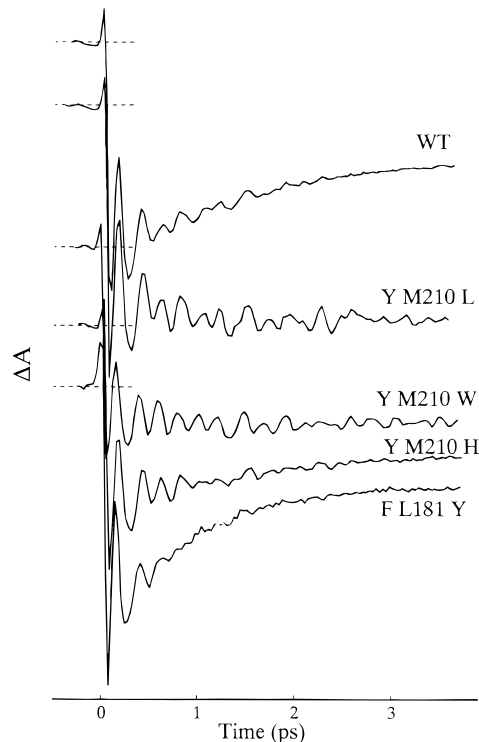


FIGURE 2: 10 K transient kinetics at the blue side of the emission band (at 907 nm).

picoseconds (Figure 1, middle panel). The stimulated emission spectrum moves out of the Franck–Condon region, where ground state absorption and emission overlap, on the 100 fs time scale and subsequently oscillates as is observed in WT RCs (Vos et al., 1994a). However, in this mutant, the oscillations of the spectrum are more clearly visualized due to the separation in time scale between vibrational motions and  $P^*$  decay.

Figure 2 shows the kinetics at the blue side of the emission band, where the stimulated emission is superimposed on ground state bleaching. For all mutants, the oscillations at both extremes of the emission band are in counterphase as reported previously for WT RCs [cf. Vos et al. (1995) for the kinetics at the red side of the emission band]. The general features of the oscillations are similar for all of the mutant RCs. The FT of the oscillatory parts of the data (Figure 3) shows that the main vibrational bands at 70, 94, 125, and 148  $\text{cm}^{-1}$  observed in WT RCs are also present in all of the mutant complexes. The relative intensity of these bands and the pattern of the much weaker bands in the 180–300  $\text{cm}^{-1}$  region vary somewhat between the different mutants. We note that a small band at 336  $\text{cm}^{-1}$  in WT RCs is found reproducibly in the mutants (at 343  $\text{cm}^{-1}$  in YM210H and FL181Y).

Interestingly, the oscillations are not completely damped after 3–4 ps in the YM210L and YM210W mutants, where  $P^*$  is very long-lived (Figure 2). This is in contrast to the WT, the YM210H mutant, and especially the FL181Y mutant, in which  $P^*$  is very short-lived. Associated with the longer damping times in the YM210L and YM210W mutants is the narrowing of the vibrational bands in the FT spectrum (Figure 3). Clearly, there is a strong correlation between the damping time and the lifetime of  $P^*$ . This strongly suggests that the damping of the oscillations in WT RCs is mainly due to the depopulation of  $P^*$  and not to intrinsic vibrational dephasing.

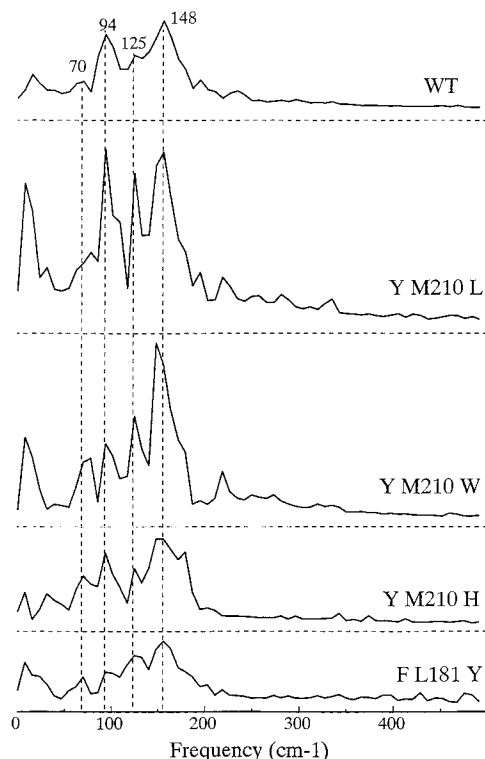


FIGURE 3: Fourier-transforms of the oscillatory parts of the data of Figure 2.

Mutants with a long-lived  $P^*$  state can be used to estimate a minimal time for vibrational dephasing due to interactions with the bath or anharmonic coupling. It should be kept in mind that the large number of close-lying modes that are activated complicates a direct estimation from the kinetics. In principle, the homogeneous width of the FT vibrational bands can be used for such an estimation, assuming that the kinetics are modulated by exponentially damped sinusoidal functions. The amplitude of the FT,  $F(\nu)$ , in the  $t > 0$  time domain of a nonsymmetrized function,  $e^{-t/\tau} \sin(2\pi\nu_0 t)$ , has the form of the square root of a Lorentzian:

$$F(\nu) \propto \sqrt{\frac{1}{1 + 4\pi^2(\nu - \nu_0)^2\tau^2}} \quad (1)$$

from which  $\tau$  can be obtained from the full width at half-maximum (fwhm)  $\Delta\nu$  with

$$\tau = \frac{\sqrt{3}}{\pi\Delta\nu} \quad (2)$$

A width of  $18 \text{ cm}^{-1}$  would correspond to a damping time of 1 ps. The limited ( $\sim 8 \text{ cm}^{-1}$ ) frequency resolution of the present experiments does not allow a very precise determination of the width of the vibrational bands. For the YM210L mutant, the  $148 \text{ cm}^{-1}$  band has a fwhm of  $\sim 15 \text{ cm}^{-1}$ , and the bands at 94 and  $125 \text{ cm}^{-1}$  have a fwhm of  $\sim 10 \text{ cm}^{-1}$  or less. The fwhm values of the smaller bands are also in the range of  $<10\text{--}20 \text{ cm}^{-1}$ . So, in the time domain, the data can be modeled with a variety of modes with damping times ranging from  $\sim 1.2$  to 2 ps or more. In addition to the homogeneous broadening discussed above, the vibrational bands can be broadened inhomogeneously by frequency dispersion and also by congestion of overlapping bands. Therefore, the extracted damping times should be

regarded as *lower limits* for the true dephasing times of the modes under study. Summarising, the vibrational dephasing at 10 K of the activated modes, takes place on a time scale of at least 2 ps for most modes and the dephasing efficiency may be mode-dependent.

At room temperature, oscillations in mutant RCs were also found to be similar to those in WT (not shown). However, due to a less well-defined initial phase of the wave packet, the relative amplitude of the oscillations strongly diminishes at room temperature, as documented previously for WT RCs (Vos et al., 1994b). This presently prevents a detailed analysis of the damping beyond  $\sim 1\text{--}1.5$  ps.

## DISCUSSION

**Overall ET Kinetics.** The overall kinetics of  $P^*$  decay in the membrane-bound mutant RCs reported here are in general agreement with earlier studies on detergent-solubilized RCs bearing similar mutations, but under experimental conditions where coherence effects were not observed (Nagarajan et al., 1993; Jia et al., 1993; Hamm et al., 1993). For the YM210L and YM210W mutants, the decay in the bleach of the  $P$  absorption band indicates that the overall decay of the  $P^*$  state corresponds to a combination of ET and direct decay to the ground state. The latter process thus occurs in the hundreds of picoseconds time range in these mutants at 10 K. This is in general agreement with previous measurements on the ET-impaired  $D_{LL}$  mutant of *R. capsulatus*, where decay of  $P^*$  to the ground state was found to occur on the same time scale at room temperature (Breton et al., 1990) as well as at low temperature (unpublished results). Curiously, Nagarajan et al. (1993), when studying isolated RCs of the YM210W mutant, found a reduced quantum yield (80%) at room temperature, but not at 80 K, where ET was slowed down to 155 ps. This trend seems to contrast with our estimate for the quantum yield of  $\sim 50\%$  at 10 K. The origin of this contrast remains to be clarified.

At the other extreme, we found a main overall decay of  $\sim 0.7$  ps at the center of the emission band at 10 K for the FL181Y mutant. As expected from earlier measurements of comparable mutants, this is faster than in WT RCs (Jia et al., 1993; Hamm et al., 1993). It is also somewhat faster than the value of 1.3 ps reported for the stimulated emission decay at 910 nm in isolated RCs from the equivalent mutant in *R. capsulatus* at 17 K (Jia et al., 1993).

**Transient Electronic Spectra.** The pronounced structure of the transient bleaching/stimulated emission spectra (with apparent minima at  $\sim 895$ , 910, and 925 nm), observed previously only on the time scale of up to a few picoseconds for WT RCs (Vos et al., 1994a), is present also at the 100 ps time scale in the mutants with a long-lived  $P^*$  state and disappears with the decay of  $P^*$ . These features probably arise from the superposition of the bleaching of a steep ground state band and a steep stimulated emission band as is explained elsewhere (Vos et al., 1995). The long delay times, up to at least 300 ps, at which these features are still present make our previous tentative explanation (Vos et al., 1994a) in terms of a vibrationally unrelaxed excited state unlikely.

**Vibrational Spectra.** In agreement with an earlier comparison of the kinetics of spontaneous emission on isolated RCs of the YM210F mutant and WT (Stanley & Boxer, 1995), the FT vibrational spectra of the membrane-bound

mutant RCs in this study are similar to those of WT RCs. In particular, the main bands in the 50–150  $\text{cm}^{-1}$  region are found at the same positions for the mutants and for the WT. This implies that, if the protein backbone is involved in these vibrational modes, modification of a single residue (at least Tyr M210 or Phe L181) does not alter the frequencies of the modes to a significant extent. This is consistent with a picture in which these modes involve extended regions of the protein, as discussed previously (Vos et al., 1994a). Our observations are in principle also consistent with a very localized character in which only chromophores are involved in these vibrational modes. However, especially for the very low-frequency modes ( $<100 \text{ cm}^{-1}$ ), such an origin seems less likely. Although low-frequency modes have recently also been observed for dry bacteriochlorophyll (T. A. Mattioli, personal communication; Lutz, 1995; Diers & Bocian, 1995), comparison with the vibrational modes observed in RCs also indicates that the protein environment influences those modes.

The observed similarities between the FT spectra of the various complexes also imply that the identities of the residues at positions M210 and L181 do not significantly influence the structure of the cofactor system, as is also indicated by the very similar ground state absorption spectra of these mutants (Jones et al., 1994). A different situation applies when residues involved in hydrogen bonding to P are modified (to be published).

The amplitude distribution of the different vibrational modes presumably reflects the distribution of the electron–phonon couplings of the various modes, and consequently the charge distribution over the cofactors in the  $\text{P}^*$  state. In this study, the relative amplitudes of the vibrational modes display some variation, which is mainly apparent for the YM210W mutant, and hence the charge distribution within  $\text{P}^*$  may vary somewhat. The variation is very small among YM210L, YM210H, and WT RCs. From a recent FT–Raman study, it was concluded that for the  $\text{P}^+$  state of the latter set, the charge distribution over the two bacteriochlorophylls constituting P is essentially unchanged (Jones et al., 1994). Although this is an interesting observation, it should be stressed that there is *a priori* no indication that the charge distributions in  $\text{P}^*$  and in  $\text{P}^+$  are directly related.

Higher frequency vibrational modes may be expected to be more sensitive to single site mutations in the near vicinity of P than the lowest frequency modes. This may explain the relatively large differences between the mutants observed in the higher frequency (180–350  $\text{cm}^{-1}$ ) region. The very small but reproducible feature near 336  $\text{cm}^{-1}$  present in all the mutants probably corresponds to a Raman mode at 332  $\text{cm}^{-1}$  observed at room temperature when exciting in resonance with both P and the B bacteriochlorophyll monomers (Cherepy et al., 1994; Palaniappan et al., 1995) and at 340  $\text{cm}^{-1}$  in FT–Raman when exciting in preresonance with P at cryogenic temperature (T. A. Mattioli, personal communication). This feature may reflect an internal bacteriochlorophyll mode.

It remains to be established if and how the light-activated vibrational motions are involved in the primary charge separation process. It is tempting to speculate on the observation in the present study that it is possible to modify the ET properties in these mutants without strongly modifying the vibrational patterns. However, whereas the vibrational spectra associated with coherent nuclear motion of the

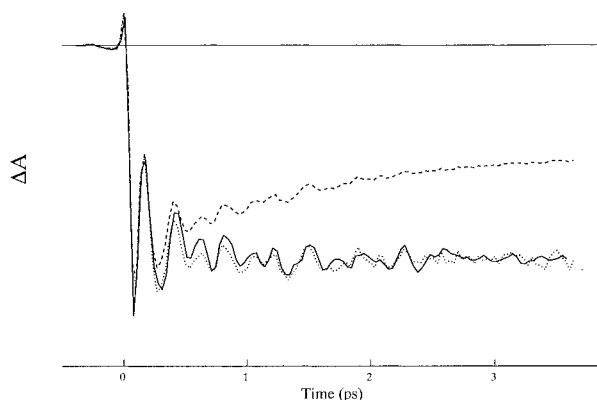


FIGURE 4: 10 K kinetics at 907 nm for the YM210L mutant (solid) and WT (dashed) RCs. The dotted curve represents the data of the dashed curve in which the decaying part was divided by the biexponential fit of the decaying part as described in the text.

RC mutants studied here are rather similar, their electronic properties are known to vary. For instance, the  $\text{P}^+/\text{P}$  redox potential in the FL181Y mutant of *R. capsulatus* has been reported to be  $\sim 25 \text{ mV}$  below that of the WT (Jia et al., 1993). For membrane-bound RCs of the YM210W and YM210L mutants, the  $\text{P}^+/\text{P}$  redox potential lies approximately 55 and 30 mV above that of WT membrane-bound RCs, respectively, while that of YM210H lies approximately 40 mV below that of WT RCs (Beekman et al., 1996). For the YM210W mutant, the free energy gap between  $\text{P}^*$  and  $\text{P}^+\text{H}_\text{L}^-$  was also reported to be diminished by  $\sim 50\text{--}70 \text{ meV}$  (Nagarajan et al., 1993). In addition to the energy levels, the electronic couplings between the different levels may be influenced by mutations at positions M210 and L181. Therefore, the apparent lack of correlation between the time scale of ET and activated vibrational modes in these particular mutants cannot be taken as evidence that these modes are not directly involved in the ET process. Even in the case that the “reaction coordinate” to the transition zone between  $\text{P}^*$  and  $\text{P}^+$  is along one or more of the activated coherent modes, the probability of transition from that zone will depend on the electronic parameters of the system.

**Vibrational Dephasing.** The rate of damping of the oscillations in the set of RCs studied here occurred in the order (fast to slow) FL181Y, WT and YM210H, YM210L and YM210W, which is the same order as the overall decay of the  $\text{P}^*$  state. Thus, the damping of the oscillatory features is clearly related to the time scale in which primary ET occurs. This is in agreement with the evidence that the vibrational motions underlying the oscillatory features take place on the  $\text{P}^*$  potential energy surface (Vos et al., 1993, 1994a). For the FL181Y and YM210H mutants and the WT RCs, this implies that the damping is primarily due to the depopulation of the  $\text{P}^*$  state and *not* primarily to vibrational dephasing or relaxation by interactions with the bath.

This point is further illustrated in Figure 4, where we have tried to “construct” oscillations in WT RCs in the hypothetical absence of ET in the following way. The data  $[\Delta A(t)]$  were fitted with a biexponential decay function  $[D(t)]$  and an asymptote ( $\Delta A_\infty$ ). The “reconstituted” data  $[R(t)]$  are then obtained by dividing the presumed decaying part of the data by the fit:

$$R(t) = \frac{\Delta A(t) - \Delta A_\infty}{D(t)} + \Delta A_\infty \quad (3)$$

In this manner, the influence of the decay of  $P^*$  on the amplitude of the oscillations is approximately balanced. Of course, the exponential fit through the oscillations is somewhat arbitrary, and the kinetics of ET may be nonexponential, but this will not influence a general comparison of the amplitudes of the oscillatory features. From Figure 4, it is clear that both the vibrational pattern and the damping of the oscillations are very similar in the constructed pattern in WT RCs (dotted line) and in the measured pattern in the YM210L mutant (solid line). This analysis supports our conclusion that the disappearance of the oscillations in WT is mainly due to decay of the  $P^*$  state. Furthermore, the YM210L mutant appears to constitute a good model system, in which the properties of the activated vibrational motions are very close to those of the WT RC. In particular, such a model may be useful in future studies for evaluating the influence of  $P^*$  vibrational motions in other spectral regions where contributions arising from  $P^*$  may overlap with those of product states.

In some very recent work on other proteins, notably light-harvesting proteins (Chachisvilis et al., 1994; Savikhin et al., 1994) and heme proteins (Zhu et al., 1994), low-frequency oscillations were reported with damping times substantially less than 1 ps. In these cases, the damping may also (partially) be due to decay of the electronic state in which the vibrational coherences are initially created, in a similar way as we have found to be the case for WT RCs.

A major observation from this work concerns the mutant RCs where coherence lifetimes are not determined by decay of the  $P^*$  state. In these complexes, the oscillations are not completely damped after 3–4 ps, and the vibrational dephasing times for most activated modes are at least  $\sim 2$  ps at 10 K and at least  $\sim 1$  ps at room temperature. As it can be expected that vibrational dephasing is more efficient at higher temperatures, this indicates that most of the dephasing, at least at low temperature, probably occurs on a longer time scale than  $\sim 2$  ps.

In summary, the lower limit of the intrinsic vibrational dephasing time of  $\sim 1$  ps determined on previous studies on intracytoplasmic membranes containing WT RCs (Vos et al., 1994a) has been pushed to  $\sim 2$  ps for most modes in the present work. This implies that intraprotein interactions leading to destruction of phase relationships and thermalization of the light-activated modes take place on a time scale which is at least that of primary ET. Our results on the intrinsic vibrational dephasing in RCs are in qualitative agreement with modelling of neutron scattering data (Smith et al., 1990) and temperature echo molecular dynamics simulations (Becker & Karplus, 1993), both on bovine pancreas trypsin inhibitor, which indicate that the ensemble of the thermally populated modes above  $\sim 15$   $\text{cm}^{-1}$  are underdamped. However, in our studies, and more generally upon external triggering of a biological reaction, the system is prepared in an off-equilibrium configuration, such that a reduced number of modes are specifically activated. In this case, the other, thermally populated, protein modes can be considered as the heat bath for the coherently activated modes. In principle it is possible that dephasing occurs on different time scales for both sets of modes.

## REFERENCES

- Becker, O. M., & Karplus, M. (1993) *Phys. Rev. Lett.* 70, 3514–3517.
- Beekman, L. M. P., Visschers, R. W., Monshouwer, R., Heer-Dawson, M., Mattioli, T. A., McGlynn, P., Hunter, C. N., Robert, B., van Stokkum, I. H. M., van Grondelle, R. & Jones, M. R. (1995) *Biochemistry* 34, 14712–14721.
- Beekman, L. M. P., Monshouwer, R., Reijnders, A. J., von Stokkum, I. H. M., McGlynn, P., Visschers, R. W., Jones, M. R., & van Grondelle, R. (1996) *J. Phys. Chem.* (in press).
- Breton, J., Martin, J.-L., Lambry, J.-C., Robles, S. J., & Youvan, D. C. (1990) in *Reaction Centers of Photosynthetic Bacteria* (Michel-Beyerle, M. E., Ed.) pp 293–302, Springer, Berlin.
- Chachisvilis, M., Pullerits, T., Jones, M. R., Hunter, C. N., & Sundström, V. (1994) *Chem. Phys. Lett.* 224, 345–354.
- Chan, C.-K., Chen, L. X.-Q., DiMaggio, T. J., Hanson, D. K., Nance, S. L., Schiffer, M., Norris, J. R., & Fleming, G. R. (1991) *Chem. Phys. Lett.* 176, 366–372.
- Cherepy, N. J., Shreve, A. P., Moore, L. J., Franzen, S., Boxer, S. G., & Mathies, R. A. (1994) *J. Phys. Chem.* 98, 6023–6029.
- Diers, J. R., & Bocian, D. F. (1995) *J. Am. Chem. Soc.* 117, 6629–6630.
- Finkele, U., Lauterwasser, C., Zinth, W., Gray, K. A., & Oesterhelt, D. (1990) *Biochemistry* 29, 8517–8521.
- Gray, K. A., Farchaus, J. W., Wachtveitl, J., Breton, J., & Oesterhelt, D. A. (1990) *EMBO J.* 9, 2061–2070.
- Hamm, P., Gray, K. A., Oesterhelt, D., Feick, R., Scheer, H., & Zinth, W. (1993) *Biochim. Biophys. Acta* 1142, 99–105.
- Jean, J. M. (1994) *J. Chem. Phys.* 101, 10464–10473.
- Jia, Y., DiMaggio, T. J., Chan, C.-K., Wang, Z., Du, M., Hanson, D. K., Schiffer, M., Norris, J. R., Fleming, G. R., & Popov, M. S. (1993) *J. Phys. Chem.* 97, 13180–13191.
- Jones, M. R., Visschers, R. W., van Grondelle, R., & Hunter, C. N. (1992) *Biochemistry* 31, 4458–4465.
- Jones, M. R., Heer-Dawson, M., Mattioli, T. A., Hunter, C. N., & Robert, B. (1994) *FEBS Lett.* 339, 18–24.
- Lutz, M. (1995) *Biospectroscopy* 1, 313–327.
- Nagarajan, V., Parson, W. W., Gaul, D., & Schenck, C. (1990) *Proc. Natl. Acad. Sci. U.S.A.* 87, 7888–7892.
- Nagarajan, V., Parson, W. W., Davis, D., & Schenck, C. (1993) *Biochemistry* 32, 12324–12336.
- Palaniappan, V., Schenck, C. C., & Bocian, D. F. (1995) *J. Phys. Chem.* 99, 17049–17058.
- Peloquin, J. M., Lin, S., Taguchi, A. K. W., & Woodbury, N. W. (1995) *J. Phys. Chem.* 99, 1349–1356.
- Savikhin, S., Zhu, Y., Lin, S., Blankenship, R. E., & Struve, W. S. (1994) in *Ultrafast Phenomena IX* (Barbara, P. F., Knox, W. H., Mourou, G. A., & Zewail, A. H., Eds.) pp 427–429, Springer, Berlin.
- Shochat, S., Arlt, T., Francke, C., Gast, P., van Noort, P. I., Otte, S. C. M., Schelvis, H. P. M., Schmidt, S., Vijgenboom, E., Vrieze, J., Zinth, W., & Hoff, A. J. (1994) *Photosynth. Res.* 40, 55–66.
- Smith, J. C., Cusack, S., Tidor, B., & Karplus, M. (1990) *J. Chem. Phys.* 93, 2974–2991.
- Stanley, R. J., & Boxer, S. G. (1995) *J. Phys. Chem.* 99, 859–863.
- Vos, M. H., Lambry, J.-C., Robles, S. J., Youvan, D. G., Breton, J., & Martin, J.-L. (1991) *Proc. Natl. Acad. Sci. U.S.A.* 88, 8885–8889.
- Vos, M. H., Rappaport, F., Lambry, J.-C., Breton, J., & Martin, J.-L. (1993) *Nature* 363, 320–325.
- Vos, M. H., Jones, M. R., Hunter, C. N., Breton, J., Lambry, J.-C., & Martin, J.-L. (1994a) *Biochemistry* 33, 6750–6757.
- Vos, M. H., Jones, M. R., Hunter, C. N., Breton, J., & Martin, J.-L. (1994b) *Proc. Natl. Acad. Sci. U.S.A.* 91, 12701–12705.
- Vos, M. H., Jones, M. R., McGlynn, P., Hunter, C. N., Breton, J., & Martin, J.-L. (1994c) *Biochim. Biophys. Acta* 1186, 117–122.
- Vos, M. H., Jones, M. R., Hunter, C. N., Breton, J., Lambry, J.-C., & Martin, J.-L. (1995) in *Reaction Centers of Photosynthetic Bacteria, Structure and Dynamics* (Michel-Beyerle, M. E., Ed.) (in press), Springer, Berlin.
- Wang, Q., Schoenlein, R. W., Peteanu, L. A., Mathies, R. A., & Shank, C. V. (1994) *Science* 266, 422–424.
- Zhu, L., Li, P., Huang, M., Sage, J. T., & Champion, P. M. (1994) *Phys. Rev. Lett.* 72, 301–304.